

Pseudo-Goldstone excitations in chiral Yukawa-theories with quadratic explicit symmetry breaking

A. Jakovác, I. Kaposvári, and A. Patkós

Institute of Physics, Eötvös University, H-1117 Budapest, Hungary

(Received 3 March 2017; published 30 October 2017)

The symmetry breakdown pattern is studied in models containing one fermion flavor multiplet and a multicomponent scalar field, supplemented with a chiral Yukawa-interaction, and in presence of an explicit symmetry breaking source quadratic in the scalar field. In a detailed investigation of the model with $U_L(1) \times U_R(1)$ chiral symmetry, it is shown that by diminishing the strength of quadratic explicit symmetry breaking, one can still keep stable the mass ratio of the fermionic and the pseudo-Goldstone excitation. At the same time, the mass ratio of the two bosonic excitations appears to approach a unique limiting value depending only on the infrared value of the first ratio but not on the microscopic (ultraviolet) coupling values. These observations receive a general interpretation by the existence of a slowly drifting partial fixed line located in the symmetric phase. Understanding the general conditions for its existence allows the construction of a similar theory with $U_L(2) \times U_R(2)$ chiral symmetry. All results of the present investigation were obtained with a nonperturbative functional renormalization group technique making use of the first two approximations to the gradient expansion of the effective action.

DOI: [10.1103/PhysRevD.96.076018](https://doi.org/10.1103/PhysRevD.96.076018)

I. INTRODUCTION

Spontaneous symmetry breaking is a central feature of elementary particle physics. The breakdown of the $SU_L(2) \times SU_R(2)$ chiral symmetry of strong interactions results in the existence of light pseudo-Goldstone pions [1]. Their nonzero mass is usually attributed to the presence of an explicit symmetry breaking term in the Lagrangian of the effective meson theory, linear in the meson fields. In case of electroweak interactions, the would-be-Goldstone degrees of freedom transmute into the longitudinal polarization modes of the massive vector fields without any need for explicit symmetry breaking. In this case, however, the lightness of the Higgs particle awaits some dynamical explanation, in particular, since its tree level value would be seriously altered by the quadratically divergent ultraviolet field fluctuations. By the example of the strong interactions, a popular idea is to assume that the Higgs boson itself is a pseudo-Goldstone excitation of some symmetry hiding the secret of the electroweak symmetry breaking [2].

In the present paper, we shall investigate the effect of quantum fluctuations on the particle spectra when the explicit symmetry breaking is quadratic in the meson fields, instead of the conventional linear external field. The strength of this quadratic breaking itself is scale dependent, and we will be particularly interested in investigating its effect on the renormalization evolution when its starting (microscopic) value is chosen many orders of magnitude smaller than the value of the parameters preserving the symmetry of the respective models.

A model containing a real scalar (the ‘‘Higgs’’ boson) and a single fermion flavor (the ‘‘top’’) represents a minimal

framework, which allows us to study the influence of quantum fluctuations on the Higgs potential [3–13]. Though it possesses only a discrete remnant of the chiral symmetry, still an acceptable order of magnitude estimate could have been obtained for the maximal momentum value up to which the system is stable, and its characteristic data (the vacuum expectation of the scalar field, the masses of the top, and of the Higgs boson) can be fixed to their experimental values. In the present study, we make use of the simplest extension of this toy model allowing us to define the Higgs as the pseudo-Goldstone boson in the broken phase of the global continuous symmetry characterizing the extension.

The simplest extension is to replace the real scalar by a complex one and couple it to the single fermion flavor with a chiral Yukawa interaction. This model has a $U_L(1) \times U_R(1)$ global chiral symmetry, and the symmetry breaking pattern $U_L(1) \times U_R(1) \rightarrow U_V(1)$ will be studied in presence of an explicit symmetry breaking term in the effective action. This term, however, will be quadratic in the complex scalar field [14,15], in contrast to the commonly assumed linear dependence.

Model systems with an Abelian continuous symmetry have received constant interest in the past. The symmetric part of the Lagrangian has the same symmetry as the chiral one-flavor NJL model, which served as the most transparent illustration of the symmetry breaking mechanism proposed in the classic publication of Nambu and Jona-Lasinio [1]. It has been exploited as the simplest example of dynamical fermion mass generation in discussions of chiral symmetry breaking in hadrons and nuclei at finite temperature and baryonic density [16]. Detailed investigations of

its fixed point structure were realized with emphasis on the Fierz ambiguity of the parametrization of its effective action [17,18]. Its bosonization with help of a Hubbard-Stratonovich (HS) transformation [19,20] leads to a Yukawa-type model rather similar to the one investigated in this paper. The complex scalar field is of an auxiliary nature; it stands for a bound fermion-anti-fermion state. It has no proper dynamics at the scale, where the HS-transformation is applied, though field fluctuations generate in the infrared a kinetic term and also higher powers of the field in its potential energy.

It can be noted that the compositeness scale defined in [21,22] through the vanishing of the wave function renormalization constant of the scalar field could be included also into the present discussion by applying existing renormalization group techniques [23,24]. The assumed large amplitude evolution of the field renormalization (the anomalous dimension) of the scalar field due to the strong Yukawa interaction between the scalar and the fermion field was the idea behind the suggestion of the composite ($t - \bar{t}$ bound state) nature of the Higgs field. Top-quark condensation was one of the first suggestions [21,22,25,26] for the mechanism of the electroweak symmetry breaking.

Another potential physical application of the $U(1)$ -symmetric Yukawa model is the Frogatt-Nielsen mechanism explaining the hierarchy of lepton masses [27]. The starting assumption is that different lepton flavors have different charges under a hypothetical $U(1)$ symmetry, therefore couple to different powers of the bosonic flavon field in an effective low-energy model. The mass ratios can be satisfactorily reproduced by choosing appropriate powers.

The aim of the present study is to take into account the dynamical effect of quantum fluctuations on all couplings with help of renormalization group equations (RGE) [28–30]. For a first exploration of the emerging infrared physics, the equations will be solved in the local potential approximation (LPA) and the scalar potential is truncated at quartic power. The (in)sensitivity of the results to these restrictions will be discussed at length when higher powers of the potential and the effects of the wave function renormalization are switched on (the so-called LPA').

The initial (ultraviolet) strength of the explicit symmetry breaking relative to the symmetric mass term of the scalar field will be varied. This variation is hardly noticeable on the location of the critical surface separating the symmetric and broken symmetry phases of the model. At the surface, an Ising-type phase transition occurs corresponding to a $Z(2)$ -like symmetry left by the quadratic explicit symmetry breaking term. In the symmetry broken phase, the infrared spectrum will be fixed to values motivated by the known spectra of the top-Higgs sector in such a way that the pseudo-Goldstone boson of the broken $U_A(1)$ symmetry is associated with the Higgs particle. The ultraviolet strength of the explicit symmetry breaking is systematically

diminished keeping the fermion-to-pseudo-Goldstone mass ratio fixed. One finds that the heavy-boson-to-pseudo-Goldstone mass ratio is governed by the quartic self-coupling, and it approaches a unique value in the infrared irrespective of its starting ultraviolet value. The limiting value is determined by the occurrence in LPA of a line of ultraviolet fixed points in the coupling space. The fully massive fermion-boson spectrum emerging in the symmetric limiting case apparently does not follow Goldstone's theorem.

There is an obvious interest in investigating this new class of theories possessing in the leading order of the gradient expansion an interacting UV fixed line for the ultraviolet completion of quantum field theories [31]. A rather general perturbative analysis of the conditions for the existence of a UV fixed point was given recently in Ref. [32]. It was followed by a general discussion of the stability of the ground state around a UV fixed point [33] and the way symmetry breaking can be induced radiatively [34]. Existence of an interacting UV fixed point in a Yukawa-coupled system of Goldstone bosons and chiral fermions was discussed perturbatively in Ref. [35]. Necessary and sufficient conditions for asymptotic safety in general weakly coupled gauged theories were constructed [36] and collider based tests of some asymptotically safe extensions of the Standard Model were investigated [37]. Nonperturbative exploration has been achieved for a number of field theoretical models, including Yukawa-models of chiral fermions and bosons with the help of functional renormalization group equations [38–42]. It should be emphasized that the quadratic explicit symmetry breaking plays a role possibly controlling the UV quantum fluctuations even in the exact solutions of these systems.

One notes that this model with dynamically stabilized quadratic explicit symmetry breaking parameters has been discussed in the symmetric phase with the help of Dyson-Schwinger equations with all symmetry preserving couplings held fixed [14,15].

The paper is organized as follows. In Sec. II, the effective quantum action investigated in this paper is introduced and the RGE's of its couplings are presented in LPA' both in the symmetric and the broken symmetry phase based on the general Wetterich equation, supplemented with a linear cutoff function [43]. In Sec. III, the phase structure is mapped out in LPA for different initial strengths of the explicit quadratic symmetry breaking term with a quartic scalar potential. It is shown that a critical Yukawa coupling value separates the phases of broken and unbroken $U_A(1)$ symmetry for each initial set of the couplings characterizing the potential energy of the scalar field. This value is determined first from solving the RGE's with a scale independent Yukawa coupling. Next, it is argued that both the effect of the Yukawa-running and of the initial strength of the explicit symmetry breaking on the location of the

critical surface is negligible. In Sec. IV, the curves of constant pseudo-Goldstone-to-fermion mass ratios are found in the coupling space, and the accessible range of the heavy-boson-to-pseudo-Goldstone mass ratio is determined. The analysis of the mass spectra is systematically repeated upon diminishing the relative strength of the quadratic explicit symmetry breaking. The infrared value of the heavy-to-pseudo-Goldstone mass ratio appears to approach a unique limiting value. The emergence of this limiting solution is interpreted in Sec. V with the help of a line of fixed points arising in *LPA* in the symmetric phase of the theory. The stability of the fixed point structure is confirmed when higher dimensional operators with moderate strength are included into the scalar potential. In Sec. VI, the ansatz for the effective action is extended to include the effects of wave function renormalization (*LPA'*). Although the slow (logarithmic) evolution of the Yukawa coupling effaces the interacting fixed line, but remarkably only an ‘‘adiabatic drift’’ closely following the change in the *LPA* RG-flow pattern with the variation of the Yukawa coupling is produced. The *LPA* fixed line still attracts the RG trajectories from the UV region again leading to a narrowing of the range of mass ratios of the scalar masses when the strength of the explicit symmetry breaking gets weaker. A summary of our results accompanied with an outline of its possible extension to more general field theoretical models is given in Sec. VII. An appendix provides detailed explicit information on the renormalization group equations (RGE's) used in this study.

II. THE MODEL AND ITS RGE'S

The invariant part of the action is the following:

$$\begin{aligned} \Gamma_{INV} = & \int d^d x [Z_\psi \bar{\psi} \partial \psi + Z_\phi \partial_m \Phi^* \partial_m \Phi + U(\Phi^* \Phi) \\ & + h(\bar{\psi}_R \psi_L \Phi^* + \bar{\psi}_L \psi_R \Phi)], \\ \Phi = & \frac{1}{\sqrt{2}}(\Phi_1(x) + i\Phi_2(x)), \quad \psi_{R/L} = \frac{1}{2}(1 \pm \gamma_5)\psi. \end{aligned} \quad (1)$$

For the potential, one writes in the symmetric phase

$$U^{(INV)} = M^2 \Phi^* \Phi + \frac{\lambda}{6} (\Phi^* \Phi)^2 + \lambda_3 (\Phi^* \Phi)^3, \quad (2)$$

while in presence of a condensate the parametrization

$$U^{(SSB)} = \frac{\lambda}{6} \left(\Phi^* \Phi - \frac{v^2}{2} \right)^2 + \lambda_3 \left(\Phi^* \Phi - \frac{v^2}{2} \right)^3 \quad (3)$$

is more convenient. The $\sim(\Phi^* \Phi)^3$ piece, which completes the perturbatively renormalizable part of the potential, will be used in Sec. V as a small perturbation for testing the robustness of the findings obtained with quartic potential.

In other sections, we set $\lambda_3 = 0$. No attempt will be made to explore the region $\lambda < 0, \lambda_3 > 0$.

The action (1) has two global $U(1)$ symmetries. The first corresponds to the fermion number conservation,

$$\psi \rightarrow e^{i\alpha} \psi, \quad \Phi \rightarrow \Phi; \quad (4)$$

the second is generated by axial $U(1)$ transformations,

$$\psi \rightarrow e^{i\gamma_5 \Theta} \psi, \quad \bar{\psi} \rightarrow \bar{\psi} e^{i\gamma_5 \Theta}, \quad \Phi \rightarrow e^{-2i\Theta} \Phi, \quad (5)$$

which is written for the fermions of definite chiral projection as

$$\psi_L \rightarrow e^{-i\Theta} \psi_L, \quad \psi_R \rightarrow e^{i\Theta} \psi_R. \quad (6)$$

This last symmetry does not allow the presence of a chirality changing mass term for the fermions and also requires vanishing of $\Gamma_{\Phi\Phi}^{(2)} = \delta^2 \Gamma / \delta \Phi^2$ and $\Gamma_{\Phi^* \Phi^*}^{(2)} = \delta^2 \Gamma / \delta \Phi^{*2}$ in the effective action. Dynamical emergence of the corresponding terms in the course of the RG evolution corresponds to dynamical symmetry breaking (DSB) of the axial $U_A(1)$ symmetry,

$$\begin{aligned} \Gamma_{DSB} = & \int_p [\Pi \Phi(-p) \Phi(p) + \Pi^* \Phi^*(-p) \Phi^*(p)] \\ & + \int_p [\Sigma_{LR} \bar{\psi}_L(-p) \psi_R(p) + \Sigma_{RL} \bar{\psi}_R(-p) \psi_L(p)]. \end{aligned} \quad (7)$$

In the present investigation, we set $\Sigma_{RL} = \Sigma_{LR} = 0$, which means that the fermion mass is fully due to the spontaneous breaking of the $U_A(1)$ symmetry. Then there is a $Z(2)$ -like remaining discrete symmetry of the system,

$$\Phi \rightarrow -\Phi, \quad \psi_L \rightarrow i\psi_L, \quad \psi_R \rightarrow -i\psi_R. \quad (8)$$

A. RGE's of the system without scalar condensate

The Wetterich equation for a fermion-boson system can be partitioned in the following form [44,45]:

$$\begin{aligned} \partial_t \Gamma = & \frac{1}{2} \hat{\partial}_t \text{STr} \log(\Gamma^{(2)} + R_k) = -\frac{1}{2} \hat{\partial}_t \text{Tr} \log(\Gamma_F^{(2)} + R_k^F) \\ & + \frac{1}{2} \hat{\partial}_t \text{Tr} \log(\Gamma_B^{(2)} + R_k^B) \\ & + \frac{1}{2} \hat{\partial}_t \text{Tr} \log [1 - (\Gamma_B^{(2)} + R_k^B)^{-1} \Gamma_{BF}^{(2)} (\Gamma_F^{(2)} + R_k^F)^{-1} \Gamma_{FB}^{(2)}]. \end{aligned} \quad (9)$$

Here, $\Gamma^{(2)}$ denotes the full second functional derivative of the effective action, while $\Gamma_B^{(2)}$ and $\Gamma_F^{(2)}$ refer to its purely bosonic and purely fermionic sector, respectively. $\Gamma_{FB}^{(2)}$ and

$\Gamma_{BF}^{(2)}$ each contain one fermionic and one bosonic functional derivative. The last term is present when the system is immersed in a nonzero fermionic background as was discussed at length in Refs. [44,45]. It contributes to specific n -point functions defined through a number of fermionic functional derivatives even if the fermionic condensate is not present. The cutoff functions $R_k^{B/F}$ restrict the functional trace to field components with momenta larger than the actual scale k . The operation $\hat{\partial}_t = k\hat{\partial}_k$ acts only on the scale dependence of the cutoff functions $R_k^{B/F}$.

The bosonic part of $\Gamma^{(2)}$ can be written with U given in (2) in the following matrix form when one uses the row vector (Φ^*, Φ) and its adjungated column vector as independent variables:

$$\Gamma_B^{(2)}(q, q') = \frac{\delta(q + q')}{(2\pi)^d} \begin{pmatrix} Z_\phi q_R^2 + M^2 & 2\Pi^* \\ 2\Pi & Z_\phi q_R^2 + M^2 \end{pmatrix}, \quad (10)$$

where $q_R^2 = q^2 + R^B(q)$. It gives the propagator

$$G_B(q, q') = \frac{(2\pi)^d \delta(q + q')}{\Delta(q_R^2)} \begin{pmatrix} Z_\phi q_R^2 + M^2 & -2\Pi \\ -2\Pi^* & Z_\phi q_R^2 + M^2 \end{pmatrix}. \quad (11)$$

The zeros of the determinant of $\Gamma_B^{(2)}$ determine the bosonic spectra at the actual scale,

$$\begin{aligned} \Delta(q_R^2) &= (Z_\phi q_R^2 + M^2)^2 - 4|\Pi|^2, \\ m_{hb}^2 &= M^2 - 2|\Pi|, \quad m_G^2 = M^2 + 2|\Pi|. \end{aligned} \quad (12)$$

The meaning of the indices ‘‘hb’’ and ‘‘G’’ will be clarified when discussing the spontaneously broken phase. In the symmetric phase, the fermion has a massless propagator, and no mass term is generated in this phase by the quantum fluctuations either.

In the symmetric phase, the RGE’s of the parameters characterizing the quartic potential and the Yukawa interaction are the following:

$$\begin{aligned} \partial_t M^2 &= -2h^2 \int_q \hat{\partial}_t \frac{1}{Z_\psi^2 q_R^2} + \frac{2\lambda}{3} \int_q \hat{\partial}_t \frac{Z_\phi q_R^2 + M^2}{\Delta(q_R^2)}, \\ \partial_t \lambda &= 6h^4 \int_q \hat{\partial}_t \frac{1}{Z_\psi^4 q_R^4} - \frac{\lambda^2}{3} \int_q \hat{\partial}_t \frac{5(Z_\phi q_R^2 + M^2)^2 + 16|\Pi|^2}{\Delta^2(q_R^2)}, \\ \partial_t h &= h^3 \Pi \int_q \hat{\partial}_t \frac{1}{Z_\psi^2 q_R^2 \Delta(q_R^2)}. \end{aligned} \quad (13)$$

The evolution of the explicit quadratic symmetry breaking parameter is driven by itself,

$$\partial_t \Pi = -\frac{\lambda \Pi}{3} \int_q \hat{\partial}_t \frac{1}{\Delta(q_R^2)}. \quad (14)$$

The condition for the existence of the symmetric phase with vanishing scalar background $\Phi_b = \Phi_b^* = u/\sqrt{2}$ can be read off from the one-point equation,

$$\left. \frac{\delta \Gamma}{\delta \Phi} \right|_{\Phi_b} = U' \Phi_b^* + 2\Pi \Phi_b = \left(M^2 + 2\Pi + \frac{\lambda}{6} u^2 \right) \frac{u}{\sqrt{2}} = 0. \quad (15)$$

The phase transition to the broken symmetry phase occurs where $M^2 + 2\Pi$ vanishes. For this reason, it is convenient to choose $\Pi < 0$. At the phase transition, one has to change the parametrization of the potential to (3).

The $\hat{\partial}_t$ operation has been applied to the integrands of (13) and (14) with the choice of the linear (or optimized) cutoff functions [43]. Then introducing the rescaled variables

$$\begin{aligned} \Pi_r &= \frac{\Pi}{Z_\phi k^2}, \quad h_r^2 = Z_\psi^{-2} Z_\phi^{-1} h^2 k^{d-4}, \\ M_r^2 &= \frac{M^2}{Z_\phi k^2}, \quad \lambda_r = Z_\phi^{-2} \lambda k^{d-4}, \\ u_r &= Z_\phi^{1/2} u k^{(2-d)/2}, \quad v_r = Z_\phi^{1/2} v k^{(2-d)/2}, \end{aligned} \quad (16)$$

one finds the explicit expressions for the RGE’s in terms of dimensionless quantities in LPA' . The complete set, including the RG running of the anomalous dimensions η_i ,

$$\eta_\psi = -\partial_t \ln Z_\psi, \quad \eta_\phi = -\partial_t Z_\phi \quad (17)$$

is given in the Appendix.

B. RGE’s of the system with scalar condensate

The equation for the condensate takes now the form,

$$\left(\frac{\lambda}{6} (u^2 - v^2) + 2\Pi \right) \frac{u}{\sqrt{2}} = 0. \quad (18)$$

It has a positive solution for u^2 under the condition $\lambda v^2 - 12\Pi > 0$. This inequality is automatically fulfilled for negative values of Π . Below everywhere $|\Pi|$ will be displayed.

The particle spectra is determined by the following expressions:

$$\begin{aligned} \Delta(q_R^2) &= \left(Z_\phi q_R^2 + \frac{\lambda}{3} v^2 + 4|\Pi| \right) (Z_\phi q_R^2 + 4|\Pi|), \\ m_{hb}^2 &= \frac{\lambda}{3} v^2 + 4|\Pi| = \frac{\lambda}{3} u^2, \quad m_G^2 = 4|\Pi|, \quad m_\psi = h \frac{u}{\sqrt{2}}. \end{aligned} \quad (19)$$

The pseudo-Goldstone mass is given by m_G , the mass of the heavy boson is denoted by m_{hb} .

In the broken symmetry phase, the parameter v^2 replaces M^2 . In this phase, it is more convenient to solve the RG equations of the masses, where one exploits the relation $\lambda v^2/3 = m_{hb}^2 - m_G^2$ which follows (18) and (19). The RGE of $|\Pi|$ differs from that of m_G^2 only by a trivial 1/4 factor. One writes the following two equations:

$$\begin{aligned} \frac{3}{4} \partial_t m_G^2 &= -2h^2 \hat{\partial}_t \int_q \frac{1}{Z_\psi^2 q_R^2 + m_\psi^2} + \frac{\lambda}{6} \hat{\partial}_t \int_q \frac{4Z_\phi q_R^2 + m_{hb}^2 + m_G^2}{\Delta(q_R^2)}, \\ \partial_t m_{hb}^2 &= 2h^2 \hat{\partial}_t \int_q \frac{-Z_\psi^2 q_R^2 + m_\psi^2}{(Z_\psi^2 q_R^2 + m_\psi^2)^2} + \frac{\lambda}{6} \hat{\partial}_t \int_q \frac{1}{\Delta(q_R^2)} \left[4Z_\phi q_R^2 + 7m_{hb}^2 + 3m_G^2 - \frac{m_{hb}^2}{\Delta(q_R^2)} (4Z_\phi q_R^2 + m_{hb}^2 + m_G^2)^2 \right]. \end{aligned} \quad (20)$$

In order to have sufficient number of equations, one makes use of the equation of h and λ , expressing their rates through the masses. The RGE for the Yukawa coupling is the following:

$$\partial_t h = -\frac{h^3}{2} (m_{hb}^2 - m_G^2) \hat{\partial}_t \int_q \frac{-Z_\psi^2 q_R^2 + m_\psi^2}{(Z_\psi^2 q_R^2 + m_\psi^2)^2 \Delta(q_R^2)} + \frac{h^3 m_{hb}^2}{4} \hat{\partial}_t \int_q \frac{1}{Z_\psi^2 q_R^2 + m_\psi^2} \left[\frac{3}{(Z_\phi q_R^2 + m_{hb}^2)^2} - \frac{1}{(Z_\phi q_R^2 + m_G^2)^2} \right]. \quad (21)$$

The second term on the right-hand side of the equation is the result of the Φ dependence of the boson propagator and is present only in the broken symmetry phase. For the quartic coupling, the simplest is to use its original definition: $(3/2)\delta^4\Gamma/(\delta\Phi^2\delta\Phi^{*2})$. One finds a rather lengthy expression due to the complicated dependence of the determinant Δ on Φ and Φ^* . Therefore, we give its explicit expression only in the Appendix, together with the LPA' equations for the scaled (dimensionless) coupling strengths.

III. PHASE STRUCTURE IN LPA

The phase structure of the system in $d = 4$ has been mapped out in the three-dimensional coupling space of the microscopic parameters $(\lambda_\Lambda, M_{r\Lambda}^2, h_\Lambda)$ characterizing the system at the UV scale Λ . RG evolutions starting from the symmetric phase were followed to $k = 0$, since it is natural to assume that the ‘‘microscopic’’ theory is in the symmetric phase. The RG trajectory of the system was

traced for various initial ratios $|\Pi_\Lambda|/M_\Lambda^2$, and our goal was to see to what extent the resulting physical picture depends on this ratio. In the exploratory RG runs, the Yukawa coupling h was kept constant, which was a fortunate choice, since this turned out to be increasingly good approximation with diminishing the ratio $|\Pi_\Lambda|/M_\Lambda^2$. In fact, in the symmetric phase, the rate of variation of h is proportional to $\Pi(k)$ [see Eq. (13)]. The Yukawa coupling turned out to control the borderline between the symmetric and the broken $U_A(1)$ symmetry phase of the model.

A typical run is displayed in Fig. 1, for the starting ratio $|\Pi_\Lambda|/M_\Lambda^2 = 0.01$. The initial data of this run is chosen to end up at $k = 0$ with $M_0^2/\Lambda^2 = 2|\Pi_0|/\Lambda^2$, e.g., in a point on the critical surface separating the symmetric and the spontaneously broken phases as one sees when overlaying the two curves in Fig. 2. Although the small value of $|\Pi_\Lambda|/\Lambda^2$ drops by circa 2%, it is stabilized quickly and actually attracts the value of M_k^2/Λ^2 starting much higher

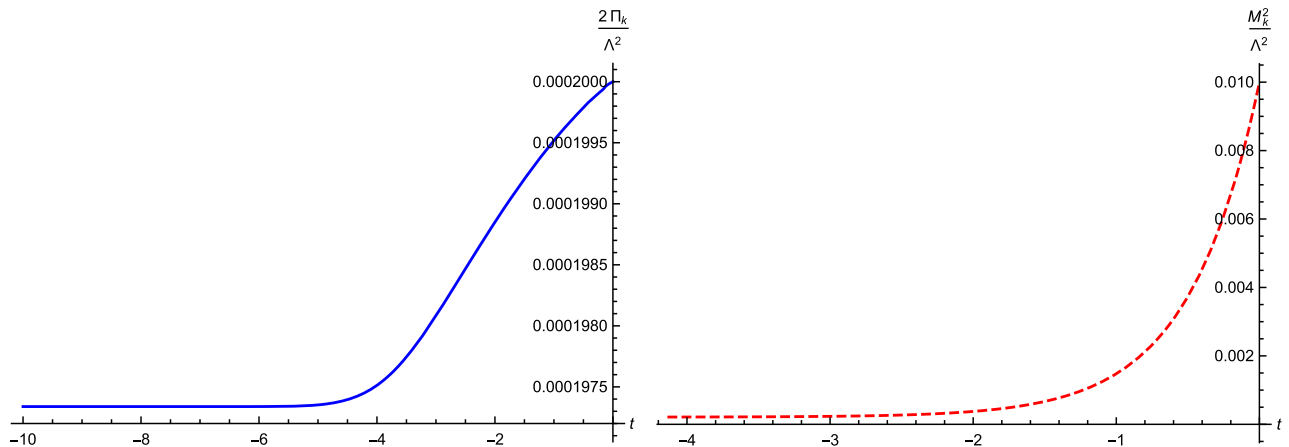


FIG. 1. A typical RG evolution of $2|\Pi|$ (left) and M^2 (right) measured in units of Λ^2 for $|\Pi_\Lambda|/M_\Lambda^2 = 0.01$.

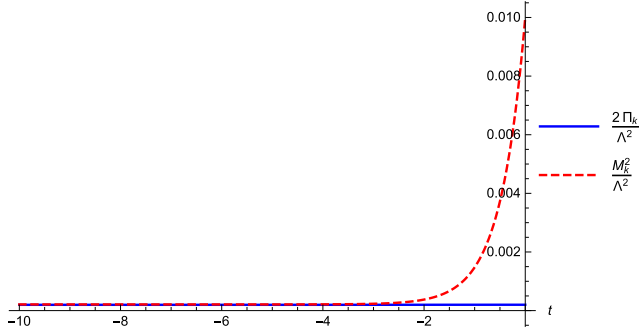


FIG. 2. An RG evolution of M^2 and $2|\Pi|$ ending on the critical surface for $|\Pi_\Lambda|/M_\Lambda^2 = 0.01$.

and steeply decreasing by the term corresponding to the quadratic divergence of the conventional perturbation theory. This qualitative behavior is universal in the sense that it is independent of the initial $|\Pi_\Lambda|/M_\Lambda^2$ ratio.

It turns out that for every initial $(M_{r\Lambda}^2, \lambda_\Lambda)$ pair, the trajectory stays in the symmetric phase when one chooses $0 < h_\Lambda < h_c(M_{r\Lambda}^2, \lambda_\Lambda)$. The critical surface $h_c(M_{r\Lambda}^2, \lambda_\Lambda)$ is displayed in Fig. 3, where the surface is cut by the “physical” value of $h_{\text{phys}} = 173/246$, corresponding to the toy Higgs-top model. Since the physical world realizes the spontaneously broken phase, the allowed region of the parameter space is nearly triangular, where $h_{\text{phys}} > h_c(M_{r\Lambda}^2, \lambda_\Lambda)$.

The variation of the surface (and also of the edge of the region belonging to the broken symmetry phase) observed

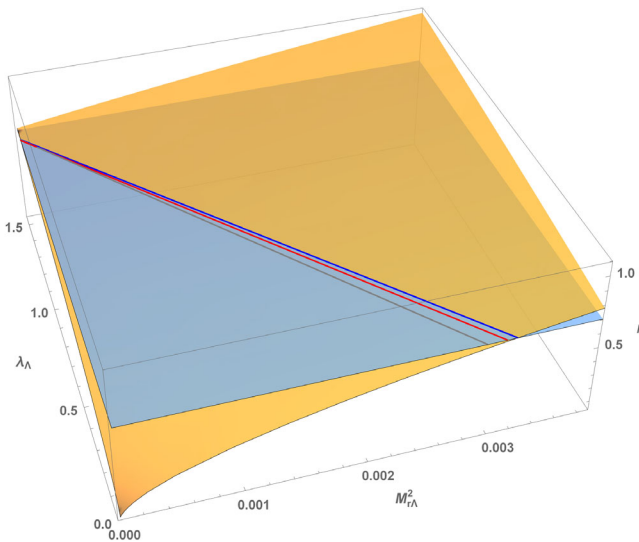


FIG. 3. The critical surface determined for the ratio $|\Pi_\Lambda|/M_\Lambda^2 = 0.01$ (yellow). The region belonging to the broken symmetry phase lies above the critical surface, the plane corresponding to the fixed value of the Yukawa coupling is colored blue. Further decreasing the value of the relative strength of the explicit symmetry breaking causes essentially no change in the shape of the critical surface. Also lines of equal infrared values of the m_G^2/m_ψ^2 ratio are displayed for two different values.

for larger values of $|\Pi_\Lambda|/M_\Lambda^2$, becomes unobservably small when $|\Pi_\Lambda|/M_\Lambda^2 \ll 0.01$ is chosen. The critical surface converges to a limiting shape essentially coinciding with the surface displayed in the figure. Also, it is important to note that the effect of the RG running of h in the final values of either $M^2(k=0)/\Lambda^2$ or $2|\Pi(k=0)|/\Lambda^2$ shows up only in the fifth decimal place.

The universality class of the phase transition can be characterized by the power of the dependence of the difference $M^2(k=0)/2|\Pi(k=0)| - 1$ on $h - h_c$, as approached from the symmetric phase. Since the lower mass in this phase has a squared mass $M^2 - 2|\Pi|$, this difference describes the infinite increase of the correlation length (the inverse mass) when the critical surface is approached. Its scaling was tested in several points of the critical surface and found to be linear, which corresponds to a critical exponent $\nu \approx 1/2$, coinciding with the mean-field value of the correlation length exponent of the Ising model. This conclusion is in agreement with the fact that the quadratic explicit symmetry breaking leaves for the full system a $Z(2)$ -like symmetry intact [see Eq. (8)].

The order parameter and the excitation spectra in the broken symmetry phase, however, reflects the $U_A(1)$ symmetry. In particular, one finds a pseudo-Goldstone-Nambu boson (PNGB) excitation in this phase. It is rather interesting that a sort of level crossing phenomenon is produced through the critical surface. The pseudo-Goldstone mode is continuously connected with the more massive mode of the symmetric phase, while the heavy mode of the broken symmetry phase develops from the critical excitation.

IV. SPECTRA OF THE BROKEN SYMMETRY PHASE IN *LPA*

As a first step of the exploration of the spectra, one can locate the starting $(\lambda_\Lambda, M_{r\Lambda}^2)$ points wherefrom a fixed infrared m_G^2/m_ψ^2 ratio can be reached. In the allowed region ($h > h_c$), which has a triangular shape when looking at it almost parallel to the h axis, these points form an almost linear curve in the $\lambda_\Lambda - M_{r\Lambda}^2$ -plane as one can see from Fig. 3. This figure is based on the RG evolutions done with $|\Pi_\Lambda|/M_\Lambda^2 = 0.01$, but its variation had not affected the qualitative features of the fixed mass-ratio curves. It is remarkable that the red-colored line which corresponds to the ratio when the pseudo-Goldstone is identified with the Higgs boson, and the fermion with the mass of the top, passes extremely close to criticality. This circumstance explains that even in the broken symmetry phase, the Yukawa coupling is hardly changing. In this region, the additional term $\sim m_{hb}^2$ of its rate of evolution is also rather small, see Eq. (21).

Next, one can investigate the ratio m_{hb}^2/m_G^2 along this line in order to see the existence of any bound for the heavy mass. The separate evolution of the two scalar masses in

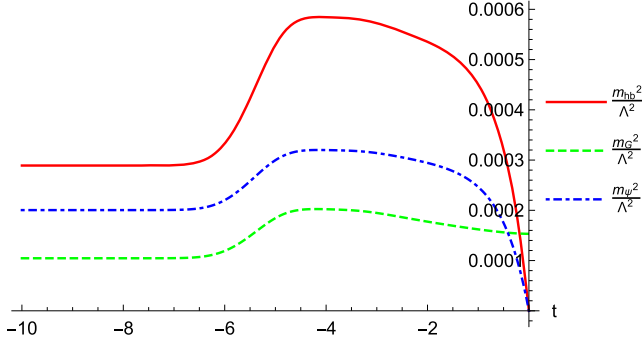


FIG. 4. RG evolution of the dimensionless squared fermion and boson masses (the PNBG is the lightest at $t = -\infty$). Note that the evolutions of the masses are displayed only in the broken symmetry phase (therefore, m_{hb}^2 and m_ψ^2 start from zero).

the broken symmetry phase displays a rather nontrivial evolution. Also the fermion (“top”) mass displays a sort of “walking” evolution around the same value of $t = \ln(k/\Lambda)$ as can be seen from Fig. 4.

The ratio m_{hb}^2/m_G^2 shows monotonic increase with decreasing $M_{r\Lambda}^2$ (or equivalently, increasing λ_Λ). Figure 5 clearly shows that there is an upper bound at the present starting $|\Pi_\Lambda|/M_\Lambda^2$ ratio.

The interesting question is to see how this upper bound modifies when the strength of the explicit symmetry breaking is systematically diminished. Since the form of the effective action is unchanged, one has for the mass ratios [see Eq. (19)],

$$\begin{aligned} \frac{m_G^2}{m_\psi^2} &= \frac{8|\Pi(k=0)|}{h^2 u^2(k=0)}, \\ \frac{m_G^2}{m_{hb}^2} &= \frac{12|\Pi(k=0)|}{\lambda(k=0)u^2(k=0)} = \frac{3h^2(k=0)}{2\lambda(k=0)} \frac{m_G^2}{m_\psi^2}. \end{aligned} \quad (22)$$

The first ratio and $m_\psi/u/\sqrt{2}$ were fixed to prescribed values. Then the variation of the second simply reflects the

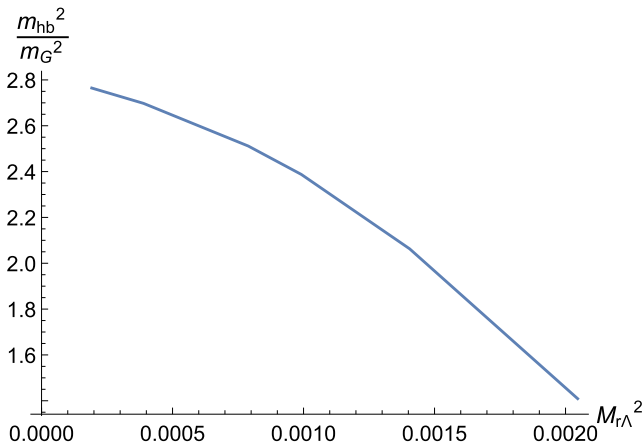


FIG. 5. Monotonic variation of the heavy-light scalar mass ratio with $M_{r\Lambda}^2$ for $|\Pi_\Lambda|/M_\Lambda^2 = .01$.

variation of $\lambda(k=0)$ with the initial data. The obvious question is to see the dependence of $\lambda(k=0)$ on Π_Λ/M_Λ^2 when its evolution starts with an arbitrary λ_Λ .

In Fig. 6, this variation is displayed in *LPA* for $\lambda_\Lambda = 0.5, 0.8, 0.94, 1.0, 1.4$ (this figure contains information also concerning the behavior in *LPA'*, which will be discussed in Sec. VI). The first thing to observe is a definite dependence with diminishing Π_Λ/M_Λ^2 in the range 10^{-3} – 10^{-7} . This is rather different from the case of the linear explicit symmetry breaking [$\sim H(\Phi + \Phi^*)$], where λ does not depend on the strength H of the explicit breaking. Actually, there is a specific λ_Λ value equal to $\lambda_s = 0.9400$, where $|\Pi_\Lambda|/M_\Lambda^2$ does not have any effect on m_G^2/m_{hb}^2 . It appears on the figure that the mass ratios arising in the region $\lambda_\Lambda > \lambda_s$ are increasing, while those falling into region $\lambda_\Lambda < \lambda_s$ decrease when the ratio $|\Pi_\Lambda|/M_\Lambda^2$ is diminished. The best fit is of the form $a + b(|\Pi_\Lambda|/M_\Lambda^2)^c$. The values $b = 0.3103$, $c = 0.0268$ were fitted, while a was fixed to the mass ratio belonging to $\lambda_\Lambda = \lambda_s = 0.9400$: $m_G^2/m_{hb}^2 \rightarrow 0.4340$. These infrared parameters vary with values of m_G^2/m_ψ^2 and of h as will be discussed shortly on an other numerical example below.

For $\lambda_\Lambda = \lambda_s$, it turns out that all couplings and masses evolve along the same RG trajectory, irrespective the starting $|\Pi_\Lambda|/M_\Lambda^2$ ratio. Just for a smaller starting value, the evolution in the symmetric phase becomes longer in t . The length of the t interval needed for the buildup of the broken symmetry characteristics is always the same. There is a mapping from the “RG time” t on the values of $|\Pi_\Lambda|/M_\Lambda^2$. This observation is the key for the RG-flow interpretation of the apparent focusing of $\lambda(k=0)$ and with it of the mass ratio m_{hb}^2/m_G^2 on a unique finite value, when the quadratic explicit symmetry breaking tends to zero.

The generic nature of the solution described above is confirmed also when one works out another parametrization suggested by the pion-sigma-constituent quark system of strong interactions. There we chose $u/\sqrt{2} \approx 100$ MeV, $m_q \approx 300$ MeV, and $m_\pi \approx 140$ MeV. The convergence to a

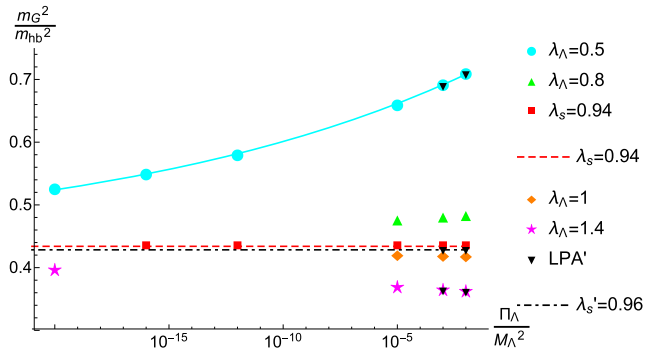


FIG. 6. Variation of m_G^2/m_{hb}^2 in *LPA* with Π_Λ/M_Λ^2 for various λ_Λ values ($h_\Lambda = 173/246$). Stability of results obtained in *LPA* is checked with *LPA'* for parameter sets, indicated in the figure (black triangles and dash-dotted black horizontal line).

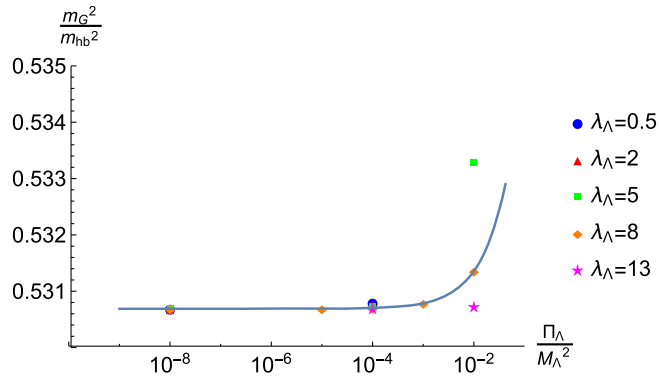


FIG. 7. Variation of m_G^2/m_{hb}^2 in *LPA* with Π_Λ/M_Λ^2 in case of parameters suggested by strong interactions ($h_\Lambda = 3$).

unique limiting m_π^2/m_σ^2 value is much faster in this case as can be seen in Fig. 7. This example is characterized by the couplings $\lambda_s \approx 17$, $h = 3$, clearly much beyond the perturbative regime. A very good power-law fit is displayed which was determined to the data: $\lambda_\Lambda = 8$, $|\Pi_\Lambda|/M_\Lambda^2 = 0.01$. The best fit parameters are $a = 0.5307$, $b = 0.0308$, $c = 0.8318$. The value of the exponent c is very different from that obtained in the previous numerical example. Its compatibility with universality is far from obvious.

At this point of the discussion, one should retain that in case of the quadratic explicit symmetry breaking, there is an alternative to the conventional picture of spontaneous symmetry breakdown in the limit of vanishing explicit breaking where one keeps the pseudo-Goldstone excitation massive (its ratio to the fermion mass is kept fixed and finite). According to this solution, the mass of its heavy boson partner is uniquely predicted in *LPA*. In the next section, it is shown that for any choice of the initial λ_Λ , the RG flow unavoidably approaches the renormalized trajectory starting from a UV fixed point λ_{UV}^* to which λ_s converges when $|\Pi_\Lambda|/M_\Lambda^2 \rightarrow 0$.

V. RG FLOW IN *LPA* FOR THE LIMITING CASE $|\Pi_\Lambda|/M_\Lambda^2 \rightarrow 0$

It can be very strange, even counterintuitive that, despite we decrease the strength of the explicit breaking, the system does not approach the spectrum expected in the phases of the fully symmetric theory. In this section, the reason for this unexpected behavior is revealed.

Let us start with an analogy that helps us to understand this phenomenon. In pure Yang-Mills theories, the only parameter that characterizes the system is the coupling constant g . It is very natural to think that a system with a large coupling is strongly interacting, while a small coupling means weak interaction, and in the zero coupling limit, the system becomes free. Still, this expectation does not work in Yang-Mills theories. If the coupling is strictly zero, there is no interaction, of course. But for an arbitrarily small positive UV value of the coupling, all choices

describe the same physics in the IR limit. The reason is that the coupling g actually depends on the scale, that is $g = g(k)$, and in the UV limit, the coupling goes to zero $g(k \rightarrow \infty) = 0$ (asymptotic freedom)—or stated another way, the system possesses an UV fixed point at $g = 0$. There is a one-to-one correspondence between the value of the coupling and the scale. This means, however, that giving the value of the coupling only tells us the scale, where we are actually looking at the system (this phenomenon is called dimensional transmutation), and has nothing to do with the strength of the interaction in the infrared.

Basically, the same dimensional transmutation occurs here in our model, with some important modifications. We have four couplings, $\lambda(k)$, $h(k)$, $\Pi(k)$, and $M^2(k)$. Their scale dependence in the symmetric phase is described in *LPA* by Eq. (A4) after putting $\eta_i = 0$. Inspecting these equations, we find that there is in the system an (interacting) UV fixed point. Assuming $M_r^2 \ll 1$ (this can be verified *a posteriori*), we arrive at the formulas

$$\frac{\lambda_{UV}^*}{h_{UV}^4} \approx \frac{18}{5}, \quad \frac{M_{r,UV}^*}{h_{UV}^2} \approx 2v_d \left(1 - \sqrt{\frac{2}{5}}\right), \quad \Pi_{r,UV}^* = 0, \quad (23)$$

while for the value of h_{UV} , we do not have any restriction, except that it still should be larger than $h_c(M_{r,\Lambda}^2, \lambda_\Lambda)$. This means that in fact we have a fixed line, not just a point.

Before continuing the analysis of the RG map, we discuss on the example of the operator $\lambda_3 \rho^3$, the persistence of the UV fixed line in *LPA*. The $\lambda_3(\Phi^* \Phi)^3$ term provides a tadpole contribution to the evolution of λ , proportional to λ_3 . The bosonic contribution to the evolution of λ_3 consists of two terms as can be checked with (A10), one is proportional to $\lambda_3 \lambda$, the other to λ^3 . There is also a fermionic contribution, Eq. (A11) proportional to h^6 . One can solve the fixed point equation of $\lambda_{3,r} = \lambda_3 k^2$ and substitute its expression into the fixed point equation of λ . For a first estimate of the effect of this term on the location of λ_{UV}^* , one can neglect the M_r^2 dependence of the new term and substitute into it for λ_{UV}^* its crude expression (23). Obviously, the whole contribution will be $\sim h^6$. Comparing this to the $\sim h^4$ term, one instantly derives an upper bound for h^2 as a negligibility condition for the $\lambda_3 \rho^3$ operator. One can look for a numerical solution of the exact fixed point equations for any given value of h . For instance, choosing $h = 173/246$, one finds $\lambda_{3,UV}^* = 5.85 \times 10^{-4}$ resulting in the following shift $\lambda_{UV}^*: 0.9400 \rightarrow 0.9450$, $M_{r,UV}^*: 1.152 \times 10^{-3} \rightarrow 1.142 \times 10^{-3}$. RG trajectories starting from the neighborhood of the new position of the fixed point will quickly find their way back to the trajectories determined with the quartic potential, since $\lambda_{3,r}$ diminishes quadratically towards the infrared.

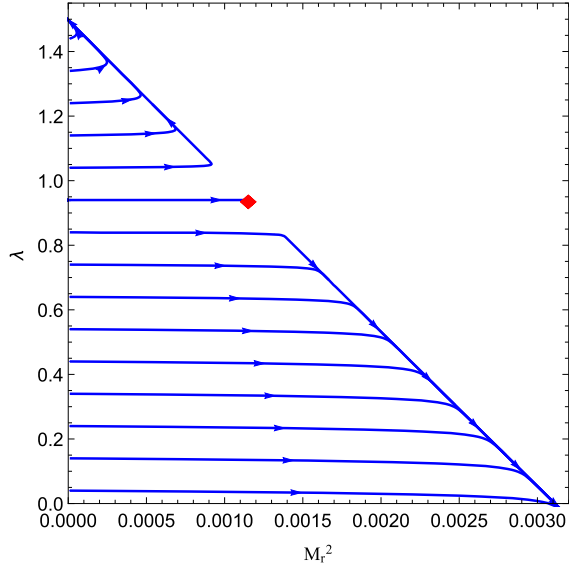


FIG. 8. Flow diagram in the $\lambda - M_r^2$ space, restricting to those initial values that lead to SSB. We can recover the UV fixed point at the analytically determined λ_{UV}^* and M_{rUV}^{*2} position (red diamond). The arrows point in the direction of increasing the RG time t . The apparent merging of the RG flows along the UV-unstable direction is fake, it is just the consequence of the finite resolution of the picture.

Let us return to the analysis of the RG map obtained with quartic scalar potential. In the $\lambda - M_r^2$ space, we can map out the flow diagram as shown in Fig. 8. In this figure, we restricted ourselves to those UV values that lead to spontaneous symmetry breaking (SSB) in the IR. We can recover the UV fixed point at some definite λ^* and M_r^{*2} position, and we see that the fixed point coordinates coincide rather well with the estimate (23) for the chosen value of h . Moreover, using the approximate expression of λ_{UV}^* in (22), one finds for the scalar mass ratio corresponding to the renormalized trajectory $m_G^2/h_{hb}^2 = 0.42$, which is in very good agreement with the numerical solution. If we are on a RG trajectory where $\lambda > \lambda_{UV}^*$, then $\lambda(k)$ will run into a Landau pole at some $k = \Lambda_L$ scale, where $M_r^2 \rightarrow -\infty$: this is the upper part of this figure. On the other hand, if we have $\lambda < \lambda_{UV}^*$ at a given scale, $\lambda(k)$ will cross zero at some $k = \Lambda_0$ value (vacuum stability bound), where $M_r^2(k)$ remains finite. We remark that although it seems from this figure that the RG trajectories merge, but this apparent phenomenon is just due to the finite resolution: two RG trajectories must never merge or cross each other.

The RG flow of Π_r is very dull: it goes to $\Pi_r = 0$ with an exponent very close to -2 , i.e., $\Pi_r(k) = C/k^2$ for large k values. But this also means that near the UV fixed point Π/M^2 scales as $\sim 1/k^2$. So, similarly to the QCD case, the quantity Π/M^2 has nothing to do with the strength of the explicit breaking, but tells us the scale, at which we look at the system.

In the above limiting process towards the vanishing of the explicit symmetry breaking, we keep λ_Λ constant, while

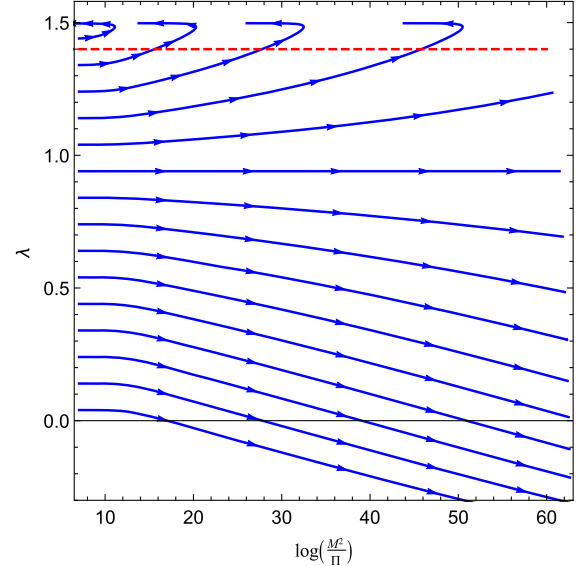


FIG. 9. RG running with increasing t in the $\lambda - \log(M^2/|\Pi|)$ plane and in the symmetric phase. The position of UV fixed point is now pushed to ∞ along the x axis. The dashed line indicates that the solution at a fixed value of λ_Λ while approaching $\Pi = 0$ forces the system to run on trajectories closer and closer to the trajectory originating from $(\lambda_{UV}^*, M_{rUV}^{*2})$.

decreasing the value of $|\Pi_\Lambda|/M_\Lambda^2$. As we have seen, $|\Pi|/M^2 \rightarrow 0$ implies increasing scale $k \rightarrow \infty$, while we keep the coupling λ_Λ fixed upon this process. But, as we also analyzed, at large scales a generic λ blows up or crosses zero, so the fact alone that at a large scale k , it is forced to assume a finite positive value, means that the RG trajectory on which it actually lies is closer and closer to the renormalized trajectory. Therefore, the corresponding IR value $\lambda(k=0)$ will converge to the one evolving along the renormalized trajectory from the fixed point value λ_{UV}^* and to the mass ratio determined by λ_{UV}^*/h_{UV}^2 .

This qualitative analysis can be followed more directly in Fig. 9, where we map the renormalization trajectories in the $\lambda - \log(M^2/|\Pi|)$ plane. In this figure, the UV fixed point is shifted to infinity. One easily recognizes that the process which increases $M_\Lambda^2/|\Pi_\Lambda|$ with λ_Λ kept fixed, singles out RG trajectories closer and closer to the renormalized trajectory originating from the point $(\lambda_{UV}^*, \log(M_{UV}^{*2}/|\Pi_{UV}^*|) = \infty)$.

For a quantitative analysis, we will assume that the above process is governed by a single UV fixed point. We introduce the usual fixed point scaling laws,

$$\delta\lambda = \lambda - \lambda_{UV}^* = (C_1 k)^{2\zeta}, \quad \delta M^2 = M_r^2 - M_{rUV}^{*2} = (C_2 k)^{-\nu}. \quad (24)$$

The powers ζ, ν' can be found by linearizing the LPA-form of the RGE's (A4) around the fixed point (23). Expanding the eigenvalues to the same order in the small quantity

$\lambda_{\text{UV}}^* v_d / (1 + M_{r\text{UV}}^{*2})^3$, the expressions for the scaling powers are the following:

$$2\zeta \approx \frac{1}{2\pi^2} \sqrt{\frac{5}{2}} h^2, \quad \nu' \approx 2 - \frac{2}{5}\zeta. \quad (25)$$

We introduce

$$\rho = \frac{M_r^2}{\Pi_r}. \quad (26)$$

Near the fixed point, at large values of ρ , we find

$$\rho \approx \frac{M_r^{*2}}{C/k^2} \sim k^2. \quad (27)$$

Therefore, near the UV fixed point, we can write

$$\delta\lambda(k) = C\rho^\zeta(k). \quad (28)$$

For smaller values of ρ , we extend its functional form as

$$\delta\lambda(k) = C(\rho(k) + \rho_0)^{\zeta(k)}. \quad (29)$$

In the IR limit, ρ runs into a constant (actually a negative value, due to SSB), and $\delta\lambda$ also reaches a constant value. Therefore, we have

$$\delta\lambda_{\text{IR}} = \delta\lambda_{\text{UV}} \frac{(\rho_{\text{IR}} + \rho_0)^{\zeta_0}}{(\rho_{\text{UV}} + \rho_0)^\zeta}. \quad (30)$$

This means that for large values of ρ_{UV}

$$\lambda_{\text{IR}} = \lambda_{\text{IR}}^* + \kappa\rho_{\text{UV}}^{-\zeta}. \quad (31)$$

This suggests a power-law approach to the limiting infrared value as was found in the numerical examples of the previous section. The above approximate expression for ζ leads to $\zeta(h = 173/246) = 0.0198$, which agrees satisfactorily with the numerically found value of the power for this case. For the second case ($h = 3$), the agreement is worse, probably because it lies beyond the perturbative regime. The increasing tendency with h^2 is qualitatively confirmed.

VI. EFFECT OF WAVE FUNCTION RENORMALIZATION (*LPA'*)

The qualitatively new effect arising from taking into account anomalous dimensions is the nontrivial evolution of the Yukawa coupling, which suppresses the existence of the interacting *LPA* fixed point in the ultraviolet. As one can see from combining (A4) with (A5) in the neighborhood of the fixed point determined in *LPA*, the variation of the Yukawa coupling is well described as

$$h_r^2(t) = \frac{h_r^2(t_0)}{1 - 2h_r^2(t_0)C(t - t_0)}, \quad C \approx v_d \left(4 + \frac{2}{1 + M_{r\text{UV}}^{*2}} \right). \quad (32)$$

This logarithmic variation is rather slow compared to the powerlike scaling of the other couplings (in particular, since $|C| < 0.02$). Therefore, one expects an ‘‘adiabatic’’ adaptation of the RG flow found in *LPA* to the actual value of $h_r(t)$, which means that the flow described for fixed $h_r(\Lambda)$ in the previous section suffers only smooth deformation as $h_r(t)$ changes.

This argument is valid near the *LPA* fixed point. More generally, one compares Fig. 8 to the flow diagram determined with *LPA'*, e.g., Fig. 10. The figure displays the flow for $|\Pi_\Lambda|/M_\Lambda^2 = 10^{-4}$, but its characteristic features do not change for weakening relative strength of the explicit symmetry breaking. Similar figures arise when $h_r(\Lambda)$ is varied.

Since there is no fixed point, the flow lines leading to the broken symmetry phase cover the complete positive quarter of the $\lambda_r - M_r^2$ plane. The most noticeable structural feature of the flow is a well recognizable remnant of the *LPA* separatrix as an almost straight line along which the RG trajectories go through a sharp (though continuous) change (see the right-hand plot in Fig. 10). Left from this line the RG trajectories essentially coincide with those found in *LPA*.

With the help of a certain λ'_s , one divides on the $\lambda_r - M_r^2$ plane the RG trajectories into two distinct classes. The trajectories which at criticality have $\lambda_r(M_r^2 = M_{r,\text{crit}}^2) < \lambda'_s(h_r(\Lambda))$ cross in the symmetric phase at some momentum scale through $\lambda_r = 0$, defining the scale of instability. Trajectories which have on the critical surface $\lambda_r(M_r^2 = M_{r,\text{crit}}^2) > \lambda'_s(h_r(\Lambda))$ eventually reach a Landau singularity. There is a borderline trajectory, clearly recognizable on the left of Fig. 10, separating these classes. This ‘‘neutral’’ trajectory is selected by choosing $\lambda_r(M_r^2 = M_{r,\text{crit}}^2) = \lambda'_s(h_r(\Lambda))$. This trajectory displays a linear $\lambda_r(M_r^2)$ dependence towards ultraviolet. The sequence of fixed points found in *LPA* also form a straight line, only with slightly different slope as one sees in Fig. 11. The moderate shift is the result of the ‘‘adiabatic’’ deformation of the trajectories.

The predetermined m_w^2/m_G^2 and $\sqrt{2}m_w/u = h_r(k=0)$ values select some $h_r(\Lambda)$ and $|\Pi_r(\Lambda)|$. The ‘‘adiabatic’’ nature of the RG-flow deformation allows us to find this initial values rather close to the *LPA* values. When one decreases $|\Pi_\Lambda|/M_\Lambda^2$, one finds the appropriate initial couplings just lying somewhat farther into UV along the *LPA'* RG trajectory.

The focusing array of RG trajectories is attracted by the neighborhood of the partial (*LPA*) fixed line labeled in the λ_r, Π_r, M_r^2 subspace by h_Λ^2 . For $\Pi_\Lambda/M_\Lambda^2 = 10^{-2} - 10^{-4}$, the initial values are rather close to the former separatrix.

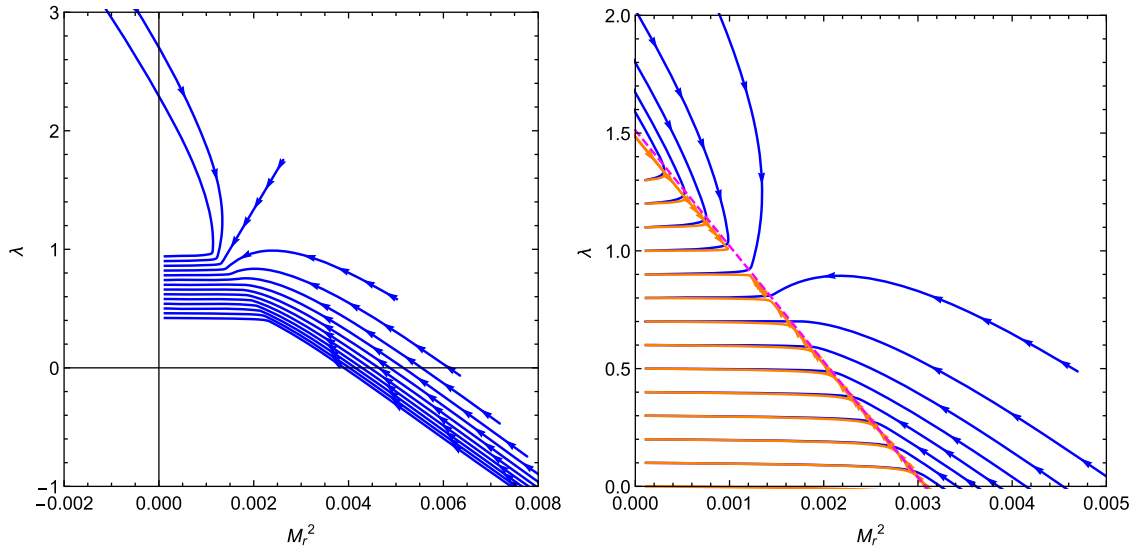


FIG. 10. Flow diagram in the $\lambda - M_r^2$ space. All trajectories start with $h_r(\Lambda) = 0.7$. There is no fixed point in LPA' , still the neighborhood of the partial (LPA) fixed point attracts the trajectories from the whole positive quarter. *Left*: The trajectory separating the regions of UV instability from that of trajectories ending in a Landau singularity is clearly recognizable. *Right*: Magnified figure allows the comparison of the RG trajectories derived in LPA (orange) and LPA' (blue). It emphasizes the close coincidence of the LPA -phase-separatrix (dashed red straight line) with the set of points where a sharp change in the character of the LPA' flow occurs. The arrows lead the eyes along the evolution towards infrared.

The effect of the wave function renormalization is minimal (η_i are both rather small) along the trajectory. Therefore, the LPA' predictions for the mass ratio m_G/m_{hb} are almost indistinguishable from the LPA results. This can be seen

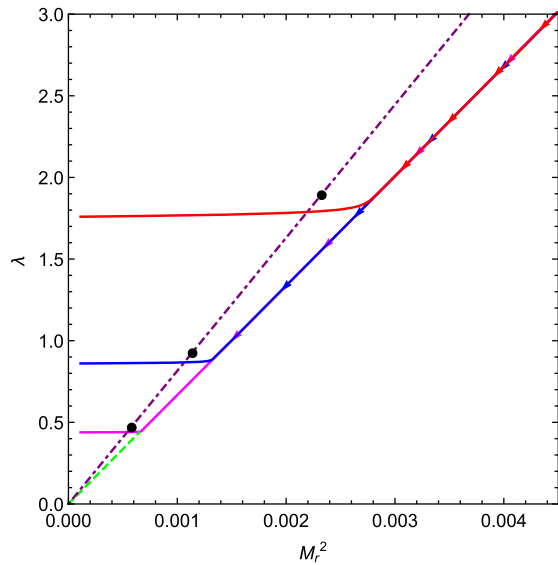


FIG. 11. The trajectories taking the same $M^2 = 2|\Pi|$ and h_r^2 values, but different λ_r , at the critical surface reach the “neutral” line in the $\lambda - M_r^2$ plane at different h_r . Next to the branching points also the LPA fixed points corresponding to these h_r values are displayed. Points of the partial LPA fixed line (see the dash-dotted line) as well as of the “neutral” line are labeled by the value of the Yukawa coupling. The two lines nearly coincide for lower values of h_r .

clearly in Fig. 6 for $\lambda_\Lambda = 0.5, 1.4$. The mass ratio belonging to λ'_s is slightly different relative to the LPA case, as one can see comparing the two horizontal lines in the same figure.

Eventually, it can be argued that similar phenomenon can be observed for the ratio m_G/m_{hb} when weakening the relative strength of the explicit symmetry breaking what has been described above in LPA . Let us keep $\lambda_r(k = \Lambda)$ fixed at some value above $\lambda'_s(M_r^2 = M_{r,crit}^2)$. With decreasing $|\Pi_\Lambda|/M_\Lambda^2$, one moves first over to trajectories closer to the trajectory of λ'_s (the “neutral” trajectory). This means that first one approaches the mass ratio belonging to λ'_s . In contrast to LPA , now one will cross the “neutral” trajectory and the corresponding $\lambda_r(M_{r,crit})$ moves away from this line, further increasing the predicted bosonic mass ratio. However, each trajectory in this region reaches a maximum at some $M_{r,max}^2$. The chosen $\lambda_r(\Lambda)$ touches upon this turning point belonging to a certain RG trajectory. When passing beyond $M_{r,max}^2$, one crosses again trajectories lying closer and closer to the “neutral” one. When one fixes an initial λ_Λ below λ'_s , one repeats the second half of this analysis. When the starting trajectory has no maximum at all, then with decreasing $|\Pi_\Lambda|/M_{r,\Lambda}$, one approaches monotonically to the ratio belonging to the “neutral” trajectory. In view of this qualitative analysis, one expects that the ratio of the scalar masses at $k = 0$ will approach in the limit of vanishing explicit symmetry breaking the set of IR couplings reached along the continuation of the “neutral” trajectory into the broken symmetry phase. The only change relative to LPA is that the convergence is now nonmonotonic.

VII. SUMMARY OF THE RESULTS AND EXTENSIONS

In this paper, we have shown that in the local potential approximation of nonperturbative renormalization group equations a $U_L(1) \times U_R(1)$ symmetric Yukawa theory with a quadratic explicit symmetry breaking term possesses a UV fixed line in the symmetric phase, characterized by vanishing strength of the explicit symmetry breaking. It is the value of the Yukawa coupling, an RG invariant in this approximation, which parametrizes the line of fixed points in the three-dimensional $(\lambda_\Lambda, h_\Lambda, M_\Lambda^2)$ coupling space.

Although the Yukawa coupling starts to evolve logarithmically in the next order of the gradient expansion of the effective action, effacing in this way the partial fixed line, it was found that a slightly displaced neighborhood of the *LPA* fixed line $(\lambda_r^*(h_\Lambda), M_r^{2*}(h_\Lambda))$ still attracts the RG trajectories from the far ultraviolet $(\lambda_r > \lambda_r^*(h_\Lambda), M_r^2 > M_r^{2*}(h_\Lambda))$. In the region $\lambda_r < \lambda_r^*(h_\Lambda), M_r^2 < M_r^{2*}(h_\Lambda)$, the RG flow of the *LPA* and *LPA'* essentially coincide.

The mechanism behind this focusing effect is made explicit by comparing the RG flow in *LPA* and *LPA'*. It appears useful to summarize in this conclusion first the general features which lead to the existence of a partial UV fixed point and comment on the changes occurring to its effects in the next approximation steps at the end.

The UV fixed point was found in *LPA* with a quartic local potential. The part of the RG flow was mapped out which crosses the critical surface, bordering the phase of broken $U_A(1)$ symmetry. The renormalized trajectory starting from the fixed point characterized by some fixed value of h has in the symmetric phase a constant $\lambda = \lambda_s$. Above this value, flow lines of the trajectories arrive from the neighborhood of Landau poles, restricting the range of allowed momenta. Below the renormalized trajectory, the physically allowed portion of the trajectories is restricted by the stability requirement $\lambda > 0$.

An important feature is that trajectories passing near the unique fixed point of the quadratic symmetry breaking $(\Pi_r^* = 0)$, in the broken symmetry are able to sustain stable fermion-to-boson and boson-to-boson mass ratios not enforcing in the limiting case the validity of Goldstone's theorem.

The key points needed for the establishment of such an *LPA* fixed line in a certain theory are the following:

- (i) The RG evolution of the explicit quadratic symmetry breaking parameter Π is driven by itself in the symmetric phase, resulting from a convenient cancellation among the contributions from the bosons as well, as a complete cancellation of the fermionic contribution.
- (ii) The rate of the RG evolution of the Yukawa coupling h is also proportional to the explicit symmetry breaking parameter Π , resulting from a convenient cancellation among the bosonic contributions.

- (iii) The existence of the interacting *LPA* fixed point $(\lambda_{UV}^*, M_{rUV}^*)$ is made possible by the compensation of the bosonic contributions (proportional to some power of the self-coupling λ) through the fermionic contribution (proportional to the nonrunning Yukawa coupling). It is a nontrivial requirement to find this fixed point in the physically allowed range.

In order to demonstrate the generic nature of the construction leading to such a UV fixed line, we shortly demonstrate its existence in a well-known model with a larger symmetry group. Let consider the $U_L(2) \times U_R(2)$ symmetric chiral “quark-meson” theory. The bosonic fields of the model are written in a 2×2 matrix with complex elements and transform as follows:

$$U = \sigma + i\eta + (s_a + i\pi_a)\tau^a, \\ U \rightarrow U_L U U_R^\dagger, \quad U_L \in SU(2)_L, \quad U_R \in SU(2)_R. \quad (33)$$

The part of the action invariant under $U_L(2) \times U_R(2)$ is the following:

$$\Gamma_{INV} = \int_x \left[\frac{1}{4} \text{Tr} \partial_\alpha U^\dagger \partial_\alpha U + \bar{\psi} \partial \psi + V(\rho) + h(\bar{\psi}_L U \psi_R + \bar{\psi}_R U^\dagger \psi_L) \right], \quad (34)$$

with $\rho = (1/4)\text{Tr} U^\dagger U$. The fermion field $\psi_{L/R}$ represents an $SU_{L/R}(2)$ doublet. The quadratic explicit symmetry breaking is chosen in the following specific form, closed upon the RG evolution:

$$\Gamma_{DSB} = \int_x \bar{\Pi} (\text{Tr} U^2 + \text{Tr} (U^\dagger)^2). \quad (35)$$

Assuming a nonzero background for the σ field, one quickly finds the expression for $\Gamma^{(2)}$ and one proceeds to the straightforward derivation of the RGE's, noting the fact that in a pure σ background with the above explicit symmetry breaking $G_\pi = G_\eta$ in both phases and $G_s = G_\sigma$ in the symmetric phase. The RGE's for the σ and π fields in the symmetric phase ($V' = M^2, V'' = \lambda/3$) are the following:

$$\partial_t(M^2 + \bar{\Pi}) = \frac{\lambda}{3} \hat{\partial}_t \int_q (3G_\sigma + 2G_\pi) - 8h^2 \hat{\partial}_t \int_q \frac{1}{q_R^2}, \\ \partial_t(M^2 - \bar{\Pi}) = \frac{\lambda}{3} \hat{\partial}_t \int_q (2G_\sigma + 3G_\pi) - 8h^2 \hat{\partial}_t \int_q \frac{1}{q_R^2}, \quad (36)$$

or

$$\begin{aligned}\partial_t M^2 &= \frac{5\lambda}{6} \hat{\partial}_t \int_q (G_\sigma + G_\pi) - 8h^2 \hat{\partial}_t \int_q \frac{1}{q_R^2}, \\ \partial_t \bar{\Pi} &= \frac{\lambda}{6} \hat{\partial}_t \int_q (G_\sigma - G_\pi) = -\frac{\lambda \bar{\Pi}}{3} \hat{\partial}_t \int_q \frac{1}{(q_R^2 + M^2)^2 - \bar{\Pi}^2}.\end{aligned}\quad (37)$$

Clearly, the explicit symmetry breaking parameter is driven by itself, and it has the fixed point $\bar{\Pi}^* = 0$.

In the symmetric phase, only fermions contribute to the RGE of the Yukawa coupling,

$$\begin{aligned}\partial_t h &= -\frac{h^3}{3} \hat{\partial}_t \int_q \frac{1}{q_R^2} [G_\sigma - G_\eta + 3(G_S - G_\pi)] \\ &= -\frac{4}{3} h^3 \hat{\partial}_t \int_q \frac{1}{q_R^2} (G_\sigma - G_\pi),\end{aligned}\quad (38)$$

which is proportional to $\bar{\Pi}$ by the difference $G_\sigma - G_\pi$ as was the case of the RGE (21) (compare with the first two points of the general scheme). Therefore, any chosen value of h might represent a fixed point solution of M_r^2 and λ . The RGE of λ is structurally the same as was the case of the $U(1)$ symmetric theory,

$$\partial_t \lambda = 48h^4 \hat{\partial}_t \int_q \frac{1}{q_R^4} - \frac{\lambda^2}{2} \hat{\partial}_t \int_q \left(G_s^2 + \frac{4}{3} G_\pi^2 + 3G_\sigma^2 \right). \quad (39)$$

Analyzing the RGE's, one quickly finds the following approximate fixed point equations for any chosen value of h^2 valid in the ultraviolet under the condition of the negligibility of M_r^2 on the right-hand side of the RGE's:

$$\begin{aligned}\Pi_{UV}^* &= 0, \quad \frac{8}{3} \lambda_{UV}^{*2} = 48h^4, \\ 2M_{rUV}^{*2} &= 2v_d \left(8h^2 - \frac{5}{3} \lambda_{UV}^* \right),\end{aligned}\quad (40)$$

having the solution

$$\Pi_{UV}^* = 0, \quad \lambda_{UV}^* = \sqrt{18}h^2, \quad M_{rUV}^{*2} = \frac{1}{32\pi^2} (8 - 5\sqrt{2})h^2. \quad (41)$$

This solution is physical, since the bracket in the expression of M_{rUV}^{*2} is positive. It is also compatible with the condition

$$R_B(q) = q^2 \left(\frac{k^2}{q^2} - 1 \right) \Theta \left(\frac{k^2}{q^2} - 1 \right), \quad R_F(q) = q \left(\frac{k}{q} - 1 \right) \Theta \left(\frac{k^2}{q^2} - 1 \right). \quad (A1)$$

In the symmetric phase, the following basic relations are used:

$M_{rUV}^{*2} \ll 1$, and the RG flow should be rather similar in its neighborhood to that described in detail for the $U(1)$ case. The particle spectra in the broken symmetry phase is far from the phenomenologically interesting case of strong interactions; therefore, the interest of the quadratic explicit symmetry breaking is doubtful for the phenomenology of any realistic two-flavor quark-meson theory.

The generality of the constructional requirements makes it clear that including higher (perturbatively irrelevant) powers of the invariant ρ into the potential $V(\rho)$ will only slightly influence the result of the analysis for moderate values of the Yukawa coupling. The upper bound on h will depend on the algebraic structure of the model.

Nonzero anomalous dimensions (the so-called *LPA'*) efface the fixed line. Since the logarithmic evolution of the Yukawa coupling in the region of the *LPA* fixed line is parametrically slower than the scaling of the other couplings, some kind of ‘‘adiabatic’’ deformation of the RG flow found in *LPA* has a chance to occur. The coefficient governing the logarithmic variation depends on the symmetry group of the theory; therefore, this expectation should be checked numerically case by case.

Possible significance of theories, whose fully massive infrared spectra is dominated by the remnants of a partial UV fixed line in the limit of vanishing explicit symmetry breaking, for consistent ultraviolet completion should be investigated in the future systematically. It would be also of interest to reconstruct the features of this study from a purely fermionic version of this model (inverse Hubbard-Stratonovich transformation). Lattice realization of the RG evolution would provide a nonperturbative check of the findings of the present paper.

ACKNOWLEDGMENT

This research was supported by the Hungarian Research Fund under Contracts No. K104292 and No. K123815. Valuable suggestions of an unknown Referee prompting considerable expansion of the scope of the first version of this communication, are thankfully acknowledged.

APPENDIX: EXPLICIT RENORMALIZATION GROUP EQUATIONS

The RGE's were derived with the linear (optimized) cutoff functions of Litim [43],

$$\begin{aligned}\hat{\partial}_t \int_q \frac{1}{(Z_\psi^2 q_R^2 + m_\psi^2)^n} &= -2n v_d k^{d+2} \frac{1}{(Z_\psi^2 k^2 + m_\psi^2)^{n+1}} \left(1 - \frac{\eta_\psi}{d+1}\right), \\ \hat{\partial}_t \int_q \frac{1}{((Z_\phi q_R^2 + M^2)^2 - 4\Pi^2)^n} &= -4n v_d k^{d+2} \frac{Z_\phi k^2 + M^2}{((Z_\phi k^2 + M^2)^2 - 4\Pi^2)^{n+1}} \left(1 - \frac{\eta_\phi}{d+2}\right),\end{aligned}\quad (\text{A2})$$

where $v_d = S_d/(d(2\pi)^d)$ with S_d denoting the surface of the d -dimensional unit sphere. In the broken symmetry phase, the following general relation is used in the derivation of the RGE's:

$$\begin{aligned}\hat{\partial}_t \int_q G_G^l(q_R^2) G_{hb}^n(q_R^2) &= -2v_d k^{d+2} G_G^l(k^2) G_{hb}^n(k^2) (lG_G(k^2) + nG_{hb}(k^2)) \left(1 - \frac{\eta_\phi}{d+2}\right), \\ G_G(q_R^2) &= \frac{1}{Z_\Phi q_R^2 + m_G^2}, \quad G_{hb}(q_R^2) = \frac{1}{Z_\Phi q_R^2 + m_{hb}^2}.\end{aligned}\quad (\text{A3})$$

In the symmetric phase and in four dimensions [$v_4 = (32\pi^2)^{-1}$], the following set is obtained for the couplings defining the ansatz for the effective action as the sum of Γ_{INV} and Γ_{DSB} , when one takes into account wave function renormalization and a quartic scalar potential:

$$\begin{aligned}\partial_t \Pi_r + (2 - \eta_\phi) \Pi_r &= \frac{4\lambda_r \Pi_r v_4}{3} \frac{1 + M_r^2}{((1 + M_r^2)^2 - 4\Pi_r^2)^2} \left(1 - \frac{\eta_\phi}{6}\right), \\ \partial_t M_r^2 + (2 - \eta_\phi) M_r^2 &= 4h_r^2 v_4 \left(1 - \frac{\eta_\psi}{5}\right) - \frac{4\lambda_r v_4}{3} \frac{(1 + M_r^2)^2 + 4\Pi_r^2}{((1 + M_r^2)^2 - 4\Pi_r^2)^2} \left(1 - \frac{\eta_\phi}{6}\right), \\ \partial_t \lambda_r - 2\eta_\phi \lambda_r &= -24h_r^4 v_4 \left(1 - \frac{\eta_\psi}{5}\right) + \frac{4\lambda_r^2 v_d (1 + M_r^2)}{3((1 + M_r^2)^2 - 4\Pi_r^2)^3} (5(1 + M_r^2)^2 + 52\Pi_r^2) \left(1 - \frac{\eta_\phi}{6}\right), \\ \partial_t h_r^2 - (\eta_\phi + 2\eta_\psi) h_r^2 &= -\frac{4\Pi_r h_r^4 v_4}{(1 + M_r^2)^2 - 4\Pi_r^2} \left[\frac{2(1 + M_r^2)}{(1 + M_r^2)^2 - 4\Pi_r^2} \left(1 - \frac{\eta_\phi}{6}\right) + 1 - \frac{\eta_\psi}{5} \right].\end{aligned}\quad (\text{A4})$$

The algebraic equations determining the anomalous dimensions look like

$$\eta_\psi = h_r^2 v_4 \frac{(1 + M_r^2)^2 + 4\Pi_r^2}{((1 + M_r^2)^2 - 4\Pi_r^2)^2} \left(1 - \frac{\eta_\phi}{5}\right), \quad \eta_\phi = h_r^2 v_4 (4 - \eta_\psi). \quad (\text{A5})$$

A test of the robustness of the conclusions obtained in *LPA* with a quartic potential is performed by investigating the effect of the next term of the expansion of the scalar potential $\lambda_3(\Phi^* \Phi)^3 \equiv \lambda_3 \rho^3$. The determinant of $\Gamma_B^{(2)}$ supplemented with this term in *LPA* has the following expression:

$$\Delta(q_R^2, \Phi, \Phi^*) = \left(q_R^2 + M^2 + \frac{2\lambda}{3}\rho + 9\lambda_3 \rho^2\right)^2 - \left(2\Pi + \frac{\lambda}{3}\Phi^{*2} + 6\lambda_3 \rho \Phi^{*2}\right) \left(2\Pi + \frac{\lambda}{3}\Phi^2 + 6\lambda_3 \rho \Phi^2\right). \quad (\text{A6})$$

It affects the bosonic contribution to $\Gamma_{\Phi^2 \Phi^{*2}}$ and $\Gamma_{\Phi^3 \Phi^{*3}}$. The derivatives of Δ with respect to Φ and Φ^* are denoted as

$$\Delta_{nm} = \frac{\delta^{n+m} \Delta}{\delta \Phi^n \delta \Phi^{*m}}. \quad (\text{A7})$$

The nonvanishing derivatives at the origin are the following:

$$\begin{aligned}\bar{\Delta}_{11} &= \frac{4\lambda}{3}(q^2 + M^2), \quad \bar{\Delta}_{22} = 4\left(\frac{\lambda^2}{3} + 18\lambda_3(q^2 + M^2)\right), \quad \bar{\Delta}_{33} = 288\lambda\lambda_3, \\ \bar{\Delta}_{20} = \bar{\Delta}_{02} &= -\frac{4\lambda}{3}\Pi, \quad \bar{\Delta}_{31} = \bar{\Delta}_{13} = -72\lambda_3\Pi.\end{aligned}\quad (\text{A8})$$

One checks readily that the tadpole integral computed with the 6-leg term contributes to the right-hand side of $\Gamma_{\Phi^2 \Phi^{*2}}$, that is to the running of $2\lambda/3$,

$$18\lambda_3 \hat{\partial}_t \int (G_G(q_R^2) + G_{hb}(q_R^2)), \quad G_G = \frac{1}{q_R^2 + M^2 - 2\Pi}, \quad G_{hb} = \frac{1}{q_R^2 + M^2 + 2\Pi}. \quad (\text{A9})$$

Taking further two derivatives, one finds the bosonic contribution to the RGE of λ_3 (after dividing both sides by 36),

$$\hat{\partial}_t \frac{\delta^6}{\delta\Phi^3 \delta\Phi^{*3}} \frac{1}{72} \int_q \log \Delta(q_R^2, \Phi, \Phi^*) = \frac{1}{72} \hat{\partial}_t \int_q \left[\frac{\Delta_{33}}{\Delta} - \frac{3}{\Delta^2} (3\Delta_{11}\Delta_{22} + 2\Delta_{20}\Delta_{31}) + \frac{6}{\Delta^3} (2\Delta_{11}^3 + 3\Delta_{20}^2\Delta_{11}) \right]. \quad (\text{A10})$$

The fermionic contribution to $\partial_t \lambda_3$ is given with help of the massless fermion propagator G_F and the chiral projectors P_{\pm} ,

$$\begin{aligned} -\frac{1}{36} \frac{\delta^6}{\delta\Phi^3 \delta\Phi^{*3}} \hat{\partial}_t \text{Tr} \log \Gamma_F^{(2)} &= \frac{1}{3} h^6 \text{Tr} (G_F P_+ G_F P_- G_F P_+ G_F P_- G_F P_+ G_F P_-) \\ &= -\frac{2}{3} h^6 \int_q \hat{\partial}_t \frac{1}{(P_F^2(q) q^2)^3}. \end{aligned} \quad (\text{A11})$$

In the broken symmetry phase, it is convenient to introduce a separate notation for the scaled propagators in LPA' ,

$$d_G = \frac{1}{1 + \mu_G^2}, \quad d_{hb} = \frac{1}{1 + \mu_{hb}^2}, \quad d_{\psi} = \frac{1}{1 + \mu_{\psi}^2}. \quad (\text{A12})$$

One writes for the Yukawa coupling and the scaled masses after a lengthy but straightforward computation the following RGE's:

$$\mu_G^2 = \frac{m_G^2}{Z_{\phi} k^2}, \quad \mu_{hb}^2 = \frac{m_{hb}^2}{Z_{\phi} k^2}, \quad \mu_{\psi}^2 = \frac{m_{\psi}^2}{Z_{\psi} k^2} \quad (\text{A13})$$

$$\begin{aligned} \frac{3}{4} (\partial_t \mu_G^2 + (2 - \eta_{\phi}) \mu_G^2) &= 4h_r^2 v_4 d_{\psi}^2 \left(1 - \frac{\eta_{\psi}}{5}\right) - \frac{\lambda_r}{3} v_4 \left(1 - \frac{\eta_{\phi}}{6}\right) [2d_{hb}^2 + 2d_G^2 - (\mu_{hb}^2 + \mu_G^2)(2 + \mu_{hb}^2 + \mu_G^2)d_{hb}^2 d_G^2], \\ \partial_t \mu_{hb}^2 + (2 - \eta_{\phi}) \mu_{hb}^2 &= 4h_r^2 v_4 (1 - \mu_{\psi}^2) d_{\psi}^3 \left(1 - \frac{\eta_{\psi}}{5}\right) \\ &\quad - \frac{4\lambda_r}{3} v_4 \left(1 - \frac{\eta_{\phi}}{6}\right) \left[d_G^2 + \frac{3}{4} (\mu_{hb}^2 + \mu_G^2) d_G d_{hb} (d_G + d_{hb}) - 2\mu_{hb}^2 (d_{hb}^3 + d_G^3 + d_{hb} d_G (d_{hb} + d_G)) \right. \\ &\quad \left. + 4\mu_{hb}^2 (\mu_{hb}^2 + \mu_G^2) (d_{hb}^3 d_G + d_{hb} d_G^3 + d_{hb}^2 d_G^2) - \frac{\mu_{hb}^2}{2} (\mu_{hb}^2 + \mu_G^2)^2 d_{hb}^2 d_G^2 (d_{hb} + d_G) \right], \\ \partial_t h_r^2 - (\eta_{\phi} + 2\eta_{\psi}) h_r^2 &= 2h_r^4 v_4 \left[\left(1 - \frac{\eta_{\psi}}{5}\right) d_{\psi}^2 \left[\mu_{hb}^2 \left(\frac{1}{2} d_G^2 - \frac{3}{2} d_{hb}^2 - d_G d_{hb} \right) + \mu_G^2 d_G d_{hb} + 4\mu_{\psi}^2 (\mu_{hb}^2 - \mu_G^2) d_G d_{hb} d_{\psi} \right] \right. \\ &\quad \left. + \left(1 - \frac{\eta_{\phi}}{6}\right) d_{\psi} [(\mu_G^2 - \mu_{hb}^2)(1 - 2\mu_{\psi}^2 d_{\psi}) d_G d_{hb} (d_G + d_{hb}) + \mu_{hb}^2 (d_G^3 - 3d_{hb}^3)] \right]. \end{aligned} \quad (\text{A14})$$

The equations of the anomalous dimensions smoothly join those valid in the symmetric phase,

$$\begin{aligned} \eta_{\phi} &= \frac{2\lambda_r}{3} v_4 \mu_{hb}^2 \left(2d_G^2 d_{hb}^2 + \frac{1}{4} (d_G^2 + d_{hb}^2)^2 \right) + h_r^2 v_4 (1 - \mu_{\psi}^2) d_{\psi}^3 (2 - \eta_{\psi} + 2d_{\psi}), \\ \eta_{\psi} &= \frac{1}{2} h_r^2 v_4 \left(1 - \frac{\eta_{\phi}}{5} \right) d_{\psi} (d_G^2 + d_{hb}^2). \end{aligned} \quad (\text{A15})$$

The fermionic contribution to the evolution of $2\lambda/3$ is given by the fermionic quadrangle diagram,

$$\frac{2}{3} \partial_t^F \lambda = 4h^4 \hat{\partial}_t \int_p G_{\psi}^2 [1 - 4m_{\psi}^2 G_{\psi} + m_{\psi}^4 G_{\psi}^2], \quad G_{\psi} = \frac{1}{Z_{\psi} P_F^2(q^2) q^2 + m_{\psi}^2}. \quad (\text{A16})$$

The bosonic contribution is much more cumbersome therefore only a semiexplicit expression is given here with help of appropriate Φ and Φ^* derivatives of the bosonic determinant

$$\Delta(q_R^2, \Phi, \Phi^*) = \left[Z_\Phi q_R^2 + \frac{\lambda}{3} \left(2\Phi\Phi^* - \frac{v^2}{2} \right) \right]^2 - \left(2\Pi + \frac{\lambda}{3} \Phi^2 \right) \left(2\Pi + \frac{\lambda}{3} \Phi^{*2} \right). \quad (\text{A17})$$

The bosonic contribution to $2\partial_t \lambda/3$ takes the following form:

$$\begin{aligned} \frac{2}{3} \partial_t^B \lambda = \frac{1}{2} \hat{\partial}_t \int_p \left\{ \frac{\Delta_{22}}{\Delta} - \frac{1}{\Delta^2} [2\Delta_{12}\Delta_{10} + 2\Delta_{21}\Delta_{01} + 2\Delta_{11}^2 + \Delta_{20}\Delta_{02}] \right. \\ \left. + \frac{2}{\Delta^3} [\Delta_{20}\Delta_{01}^2 + \Delta_{02}\Delta_{10}^2 + 4\Delta_{11}\Delta_{10}\Delta_{01}] - \frac{6\Delta_{10}^2\Delta_{01}^2}{\Delta^4} \right\}. \end{aligned} \quad (\text{A18})$$

One finds the explicit expression when each quantity appearing on the right-hand side is evaluated at $\Phi = \Phi^* = u/\sqrt{2}$. One has to substitute the following nonzero quantities, when a quartic potential is being used:

$$\begin{aligned} \bar{\Delta}_{10} = \bar{\Delta}_{01} &= \frac{2\lambda}{3} \frac{u}{\sqrt{2}} \left[2Z_\Phi q_R^2 + \frac{\lambda}{2} u^2 - \frac{\lambda}{3} v^2 - 2\Pi \right], \\ \bar{\Delta}_{11} &= \frac{2\lambda}{3} \left[2Z_\Phi q_R^2 + \lambda u^2 - \frac{\lambda}{3} v^2 \right], \quad \bar{\Delta}_{22} = \frac{4\lambda^2}{3}, \\ \bar{\Delta}_{20} = \Delta_{02} &= \frac{\lambda}{3} (\lambda u^2 - 4\Pi), \quad \bar{\Delta}_{21} = \Delta_{12} = \frac{4\lambda^2}{3} \frac{u}{\sqrt{2}}, \\ \bar{\Delta} &= \left(Z_\Phi q_R^2 + \frac{\lambda}{3} u^2 \right) (Z_\Phi q_R^2 - 4\Pi). \end{aligned} \quad (\text{A19})$$

The relevant combinations can be expressed through the bosonic masses, taking into account that at $\Phi = \Phi^* = u/\sqrt{2}$, $\Delta_{nm} = \Delta_{mn}$,

$$\begin{aligned} \Delta &= (q_R^2 + m_{hb}^2)(q_R^2 + m_G^2), \quad \Delta_{11} = \frac{2\lambda}{3} (G_{hb}^{-1} + G_G^{-1} + m_{hb}^2), \quad \Delta_{22} = \frac{4\lambda^2}{3}, \\ \Delta_{01}^2 &= \frac{\lambda}{6} m_{hb}^2 (G_{hb}^{-1} + 3G_G^{-1})^2, \quad \Delta_{01}\Delta_{12} = \frac{2\lambda^2}{3} m_{hb}^2 (G_{hb}^{-1} + 3G_G^{-1}), \quad \Delta_{02} = \frac{\lambda}{3} (3m_{hb}^2 + m_G^2). \end{aligned} \quad (\text{A20})$$

Using these in the bosonic contribution to the RGE of λ , one can express the integrand in powers $G_{hb}^l G_G^k$ to which one easily applies the $\hat{\partial}_t$ operation.

-
- [1] Y. Nambu and G. Jona-Lasinio, *Phys. Rev.* **122**, 345 (1961).
[2] D. B. Kaplan and H. Georgi, *Phys. Lett. B* **136B**, 183 (1984).
[3] K. Holland and J. Kuti, *Nucl. Phys. B* **129–130**, 765 (2004).
[4] K. Holland, *Nucl. Phys. B* **140**, 155 (2005).
[5] Z. Fodor, K. Holland, J. Kuti, D. Negradi, and C. Schroeder, *Proc. Sci.*, LAT2007 (2007) 056.
[6] P. Gerhold and K. Jansen, *J. High Energy Phys.* **07** (2009) 025.
[7] P. Gerhold and K. Jansen, *J. High Energy Phys.* **04** (2010) 094.
[8] H. Gies, C. Gneiting, and R. Sondenheimer, *Phys. Rev. D* **89**, 045012 (2014).
[9] D. Y.-J. Chu, K. Jansen, B. Knippschild, C.-J. D. Lin, and A. Nagy, *Phys. Lett. B* **744**, 146 (2015).
[10] A. Jakováč, I. Kaposvári, and A. Patkós, *Mod. Phys. Lett. A* **32**, 1750011 (2017).
[11] J. Borchardt, H. Gies, and R. Sondenheimer, *Eur. Phys. J. C* **76**, 472 (2016).
[12] H. Gies, R. Sondenheimer, and M. Warschinke, *arXiv*: 1707.04394.
[13] H. Gies and R. Sondenheimer, *arXiv*:1708.04305.
[14] T. Brauner and J. Hosek, *Phys. Rev. D* **72**, 045007 (2005).
[15] P. Benes, T. Brauner, and J. Hosek, *Phys. Rev. D* **75**, 056003 (2007).

- [16] U. Vogl and W. Weise, *Prog. Part. Nucl. Phys.* **27**, 195 (1991).
- [17] J. Braun, *J. Phys. G* **39**, 033001 (2012).
- [18] J. Braun, M. Leonhardt, and M. Pospiech, [arXiv:170500074](https://arxiv.org/abs/170500074).
- [19] R. L. Stratonovich, *Sov. Phys. Dokl.* **2**, 416 (1958)
- [20] J. Hubbard, *Phys. Rev. Lett.* **3**, 77 (1959).
- [21] W. A. Bardeen, C. T. Hill, and M. Lindner, *Phys. Rev. D* **41**, 1647 (1990).
- [22] A. Hasenfratz, P. Hasenfratz, K. Jansen, J. Kuti, and Y. Shen, *Nucl. Phys.* **B365**, 79 (1991).
- [23] D. U. Jungnickel and C. Wetterich, *Phys. Rev. D* **53**, 5142 (1996).
- [24] H. Gies and C. Wetterich, *Phys. Rev. D* **65**, 065001 (2002).
- [25] V. A. Miransky, M. Tanabashi, and K. Yamawaki, *Phys. Lett. B* **221**, 177 (1989).
- [26] V. A. Miransky, M. Tanabashi, and K. Yamawaki, *Mod. Phys. Lett. A* **04**, 1043 (1989).
- [27] C. Froggatt and H. B. Nielsen, *Nucl. Phys.* **B147**, 277 (1979).
- [28] C. Wetterich, *Nucl. Phys.* **B352**, 529 (1991).
- [29] C. Wetterich, *Phys. Lett. B* **301**, 90 (1993).
- [30] T. Morris, *Int. J. Mod. Phys. A* **09**, 2411 (1994).
- [31] S. Weinberg, in *General Relativity: an Einstein Centenary Survey*, edited by S. W. Hawking and W. Israel (Cambridge University Press, 1979), p. 790.
- [32] D. F. Litim and F. Sannino, *J. High Energy Phys.* **12** (2014) 178.
- [33] D. F. Litim, M. Mojaza, and F. Sannino, *J. High Energy Phys.* **01** (2016) 081.
- [34] S. Abel and F. Sannino, *Phys. Rev. D* **96**, 056028 (2017).
- [35] F. Bazzocchi, M. Fabbrichesi, R. Percacci, A. Tonero, and L. Vecchi, *Phys. Lett. B* **705**, 388 (2011).
- [36] A. D. Bond and D. F. Litim, *Eur. Phys. J. C* **77**, 429 (2017); **77**, 525(E) (2017).
- [37] A. D. Bond, G. Hiller, K. Kowalska, and D. F. Litim, *J. High Energy Phys.* **08** (2017) 004.
- [38] M. M. Scherer, H. Gies, and S. Rechenberger, *Acta Phys. Pol. B Proc. Suppl.* **2**, 541 (2009).
- [39] H. Gies, S. Rechenberger, and M. M. Scherer, *Eur. Phys. J. C* **66**, 403 (2010).
- [40] J. Braun, H. Gies, and D. D. Scherer, *Phys. Rev. D* **83**, 085012 (2011).
- [41] H. Gies, S. Rechenberger, M. M. Scherer, and L. Zambelli, *Eur. Phys. J. C* **73**, 2652 (2013).
- [42] A. Jakovác, A. Patkós, and P. Pósfay, *Eur. Phys. J. C* **75**, 2 (2015).
- [43] D. Litim, *Phys. Rev. D* **64**, 105004 (2001).
- [44] A. Jakovác and A. Patkós, *Phys. Rev. D* **88**, 065008 (2013).
- [45] K.-I. Aoki, K. I. Morikawa, J. I. Sumi, H. Terao, and M. Tomoyose, *Prog. Theor. Phys.* **97**, 479 (1997).